

Representation of the plasma fluid equations in “Miller equilibrium” analytical flux surface geometry

W. M. Stacey and Cheonho Bae

Fusion Research Center and Nuclear and Radiological Engineering Program,
Georgia Institute of Technology, Atlanta, Georgia 30332-0425, USA

(Received 27 May 2009; accepted 23 June 2009; published online 3 August 2009)

The plasma fluid equations are represented explicitly in the magnetic flux surface coordinate system resulting from the analytical “Miller equilibrium” solution of the Grad–Shafranov equation. The magnetic geometry is characterized by the elongation, triangularity, and location of the displaced major radius of the flux surface. The resulting fluid equations can be solved directly without the necessity of first solving the Grad–Shafranov equation numerically to define the flux surface coordinates. © 2009 American Institute of Physics. [DOI: 10.1063/1.3177613]

I. INTRODUCTION

The “natural” coordinate system for tokamak plasma physics computations is the set of nested magnetic flux surfaces because of the striking differences in particle, momentum, and energy flows within and across these flux surfaces. In general, these flux surface coordinates must be determined by a numerical solution of the Grad–Shafranov equation. However, an analytical solution of the Grad–Shafranov equation for the equilibrium magnetic flux surface geometry in tokamaks has been developed¹ in which the flux surface is completely described by the aspect ratio, elongation, triangularity, and safety factor. By representing the equations of plasma physics directly within this analytical flux surface geometry, the numerical solution of the Grad–Shafranov equation step can be omitted from the calculation procedure. The purpose of this paper is to present the representation of the fluid equations of particle, momentum, and energy balance within this analytical flux surface coordinate system for tokamaks.

II. MILLER EQUILIBRIUM

A. Geometry

Miller *et al.*¹ derived analytical expressions for an equilibrium flux surface in a plasma, as shown in Fig. 1, with elongation κ , triangularity δ , and displaced centers $R_0(r)$, where r is the half-diameter of the plasma along the mid-plane with its center located at distance $R_0(r)$ from the toroidal centerline. The positive direction of the angle θ shown in Fig. 1 corresponds to the direction of B_θ produced by a plasma current out of the page in Fig. 1, i.e., a clockwise plasma current looking down on the tokamak.

The R and Z coordinates of this plasma are described by¹

$$R(r) = R_0(r) + r \cos[\theta + x \sin \theta] \equiv R_0(r) + r \cos \xi, \tag{1}$$

$$Z(r) = \kappa r \sin \theta,$$

where $x \equiv \sin^{-1} \delta$.

The poloidal magnetic field in such flux surface geometry is¹

$$RB_\theta = R|\nabla\phi \times \nabla\psi| = \frac{\partial\psi}{\partial r}|\nabla r| = \frac{\partial\psi}{\partial r}\kappa^{-1}\Lambda(r, \theta) \\ \equiv \frac{\frac{\partial\psi}{\partial r}\kappa^{-1}[\sin^2(\theta + x \sin \theta)(1 + x \cos \theta)^2 + \kappa^2 \cos^2 \theta]^{1/2}}{\cos(x \sin \theta) + \frac{\partial R_0}{\partial r} \cos \theta + [s_\kappa - s_\delta \cos \theta + (1 + s_\kappa)x \cos \theta] \sin \theta \sin(\theta + x \sin \theta)}, \tag{2}$$

where

$$s_\kappa = \frac{r}{\kappa} \frac{\partial \kappa}{\partial r}$$

and

$$s_\delta = r \frac{\partial \delta}{\partial r} \frac{1}{\sqrt{1 - \delta^2}}$$

account for the change in elongation and triangularity, respectively, with the radial location.

The shifted circle model (which leads to the Shafranov shift) yields¹

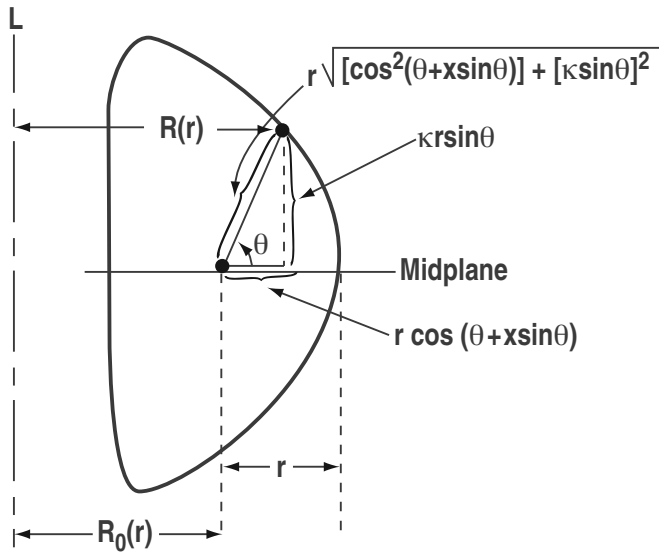


FIG. 1. Miller equilibrium geometry.

$$\frac{\partial R_0}{\partial r} \equiv \Delta' = -\frac{r}{R_0} \left(\beta_\theta + \frac{1}{2} \ell_i \right) \quad (3a)$$

and a shifted ellipse model by Lao *et al.*² yields

$$\frac{\partial R_0}{\partial r} = -\frac{r}{R_0} \left[\frac{2(\kappa^2 + 1)}{(3\kappa^2 + 1)} \left(\beta_\theta + \frac{1}{2} \ell_i \right) + \frac{1}{2} \frac{(\kappa^2 - 1)}{(3\kappa^2 + 1)} \right]. \quad (3b)$$

Here $\beta_\theta = nT/B_\theta^2/2\mu_0$ and ℓ_i is the internal inductance.

The definition of the safety factor

$$q(r) = \frac{|B_{\phi 0}|}{2\pi} \oint \frac{d\ell_\theta}{RB_\theta} \quad (4)$$

and Eq. (2) can be used to evaluate

$$\frac{\partial \psi(r)}{\partial r} = \frac{|B_{\phi 0}| \kappa(r)}{2\pi q(r)} \oint \frac{d\ell_\theta}{\left[1 + \frac{r}{R_0(r)} \cos(\theta + x \sin \theta) \right] \Lambda(r, \theta)}. \quad (5)$$

B. Flux surface coordinate system

The flux surface coordinate system is defined by the orthogonal coordinate directions (r, θ, ϕ) with length elements $d\ell_r = h_r dr$, $d\ell_\theta = h_\theta d\theta$, and $d\ell_\phi = h_\phi d\phi$. The coordinates θ and ϕ lie on the flux surface and represent a poloidal anglelike variable θ shown in Fig. 1 and the toroidal angle ϕ , respectively. The r coordinate is normal to the flux surface and can be any flux surface label—poloidal or toroidal magnetic flux, “radius,” dimensionless radius (“rho”), etc.—chosen such that the “radial” displacement is $d\ell_r = dr/|\nabla r|$. With the Miller equilibrium, the metric coefficients are

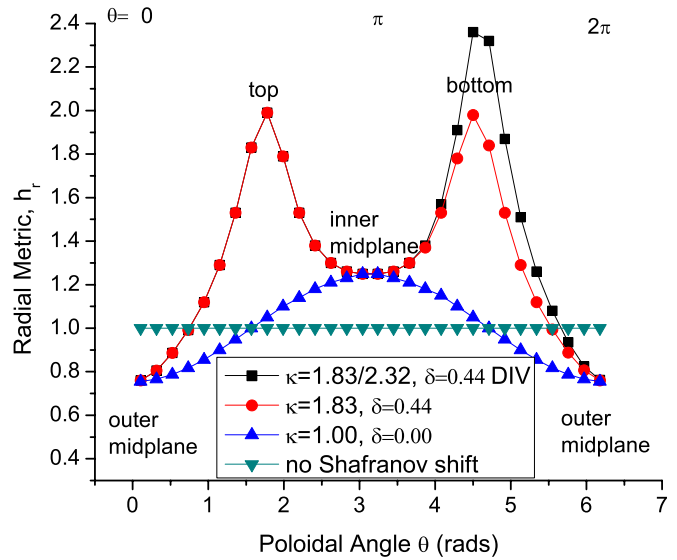


FIG. 2. (Color online) Radial metric h_r .

$$h_r = 1/|\nabla r(r, \theta)|,$$

$$h_\theta = r \sqrt{\cos^2(\theta + x \sin \theta) + \kappa^2 \sin^2 \theta}, \quad (6)$$

$$h_\phi = R_0(r) + r \cos(\theta + x \sin \theta).$$

The radial metric h_r is plotted for a flux surface just inside the last closed flux surface for the parameters of a typical DIII-D shot (but without representing the divertor) in Fig. 2 for four cases. The case shown with the downward triangles and labeled “no Shafranov shift” is plotted for a circular plasma with no Shafranov shift ($dR_0/dr=0.0$, $\kappa=1.0$, and $\delta=0.0$). The case shown with the upward triangles is the same circular plasma ($\kappa=1.0$ and $\delta=0.0$) but with Shafranov shift calculated from Eq. (3a). The case shown with the circles is an elongated plasma ($\kappa=1.83$ and $\delta=0.44$) with Shafranov shift. The case shown with squares is an elongated plasma with a lower single-null divertor represented by a larger

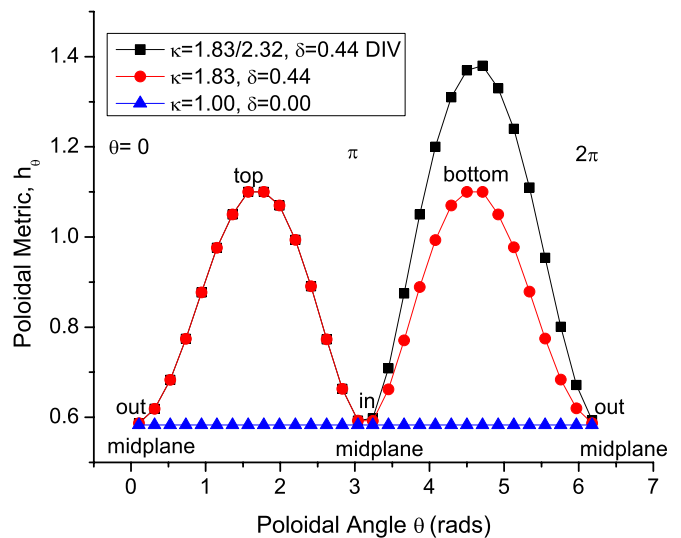


FIG. 3. (Color online) Poloidal metric h_θ .

elongation ($\kappa=2.32$) for $\pi < \theta \leq 2\pi$ than for $0 < \theta \leq \pi$. The difference in radial metric between the two circular cases (downward and upward triangles) is due to the change in $|\nabla r|$ resulting from expansion/compression of flux surfaces on the inboard/outboard resulting from the Shafranov shift. The difference in radial metric between the elongated (circles) and circular (upward triangles) cases (both with Shafranov shift) is due to the expansion of flux surfaces at the top and bottom resulting from the elongation of the plasma. Representing a lower single-null divertor (squares) by a larger lower elongation results in a greater separation between flux surfaces at the bottom than at the top.

The poloidal metric h_θ of Eq. (6) is plotted for the same three cases in Fig. 3. For the circular plasma (triangles), the metric is just the plasma radius. For an elongated plasma

with the same midplane radius, the metric is the same as for the circular plasma at the midplane but is larger by an amount, depending on the elongation at other poloidal locations.

C. Flux surface average

The flux surface average (FSA) of a quantity $A(r, \theta)$ in this flux surface geometry is

$$\langle A(r, \theta) \rangle \equiv \frac{\oint \frac{A(r, \theta) d\ell_\theta}{B_\theta}}{\oint \frac{d\ell_\theta}{B_\theta}} = \frac{\oint A(r, \theta) z(r, \theta) d\ell_\theta}{\oint z(r, \theta) d\ell_\theta}, \quad (7)$$

where

$$z(r, \theta) \equiv \frac{\cos(x \sin \theta) + \frac{\partial R_0}{\partial r} \cos \theta + [s_\kappa - s_\delta \cos \theta + (1 + s_\kappa)x \cos \theta] \sin \theta \sin(\theta + x \sin \theta)}{[\sin^2(\theta + x \sin \theta)(1 + x \cos \theta)^2 + \kappa^2 \cos^2 \theta]^{1/2} [R_0(r) + r \cos[\theta + x \sin \theta]]}. \quad (8)$$

III. DIFFERENTIAL OPERATORS IN GENERALIZED GEOMETRY

The gradient of a scalar quantity f is

$$\nabla f = \sum_i \frac{1}{h_i} \frac{\partial f}{\partial \xi_i} \mathbf{n}_i, \quad (9)$$

where the differential lengths along the coordinates ξ_i are $d\ell_i = h_i d\xi_i$ and \mathbf{n}_i denotes the unit vectors in these coordinate directions.³

The divergence of a vector \mathbf{A} is

$$\nabla \cdot \mathbf{A} = \frac{1}{H} \sum_i \frac{\partial}{\partial \xi_i} \left(\frac{H A_i}{h_i} \right), \quad (10)$$

where $H = h_1 h_2 h_3$, and the curl of \mathbf{A} has components

$$(\nabla \times \mathbf{A})_i = \sum_{j,k} \varepsilon_{ijk} \frac{1}{h_j h_k} \frac{\partial}{\partial \xi_j} (h_k A_k), \quad (11)$$

where ε_{ijk} equals +1 if $\{ijk\}$ is an even permutation of $\{123\}$, equals -1 if $\{ijk\}$ is an odd permutation of $\{123\}$, and equals 0 if $i, j,$ and k are not all different.

The directional derivative has components

$$[(\mathbf{A} \cdot \nabla) \mathbf{B}]_i = \sum_j \left(\frac{A_j}{h_j} \frac{\partial B_i}{\partial \xi_j} + \frac{A_i B_j}{h_i h_j} \frac{\partial h_i}{\partial \xi_j} - \frac{A_i B_j}{h_i h_j} \frac{\partial h_j}{\partial \xi_i} \right). \quad (12)$$

The divergence of the second-order tensor \mathbf{T} (with elements T_{ij}) has components

$$(\nabla \cdot \mathbf{T})_i = \sum_j \left[\frac{1}{H} \frac{\partial}{\partial \xi_j} \left(\frac{H T_{ji}}{h_j} \right) + \sum_l \Gamma_{il}^j T_{jl} \right], \quad (13)$$

where the Christoffel symbols are

$$\Gamma_{jk}^i = \frac{1}{h_j h_k} \left(\frac{\partial h_i}{\partial \xi_k} \delta_{ij} - \frac{\partial h_k}{\partial \xi_j} \delta_{ik} \right) \quad (14)$$

and the Kronecker delta δ_{ij} equals 1 if $i=j$ and equals 0 otherwise.

IV. FLUID EQUATIONS IN MILLER FLUX SURFACE COORDINATE SYSTEM

In this section the Braginski-type⁴ fluid equations are first written in generalized curvilinear coordinates and then specialized to the Miller flux surface geometry of Sec. II. The specific formulation of the fluid equations follows Ref. 5. While we develop the equations formally for a single ion species in the presence of electrons, the extension to multiple ion species is straightforward. We only develop the ion momentum and energy equations; there are similar equations for the electrons but with different viscosity coefficients and heating and cooling terms.⁵

A. Continuity equation

In axisymmetric geometry ($\partial/\partial\phi=0$), the continuity equation

$$\nabla \cdot n\mathbf{V} = S = n_e n_o \langle \sigma v \rangle_{\text{ion}} \equiv n_e \nu_{\text{ion}} \quad (15)$$

can be written as

$$\begin{aligned} \frac{1}{h_r} \frac{\partial}{\partial r} (nV_r) + \frac{nV_r}{h_r} \left(\frac{1}{h_\phi} \frac{\partial h_\phi}{\partial r} + \frac{1}{h_\theta} \frac{\partial h_\theta}{\partial r} \right) + \frac{1}{h_\theta} \frac{\partial}{\partial \theta} (nV_\theta) \\ + \frac{nV_\theta}{h_\theta} \left(\frac{1}{h_\phi} \frac{\partial h_\phi}{\partial \theta} + \frac{1}{h_r} \frac{\partial h_r}{\partial \theta} \right) = n_e \nu_{\text{ion}}, \end{aligned} \quad (16)$$

where the metric elements are $h_r = 1/|\nabla(r, \theta)|$, h_θ

$= r\sqrt{\cos^2(\theta+x \sin \theta)+\kappa^2 \sin^2 \theta}$ and $h_\phi=R_0(r)+r \cos(\theta+x \sin \theta)$ in the Miller equilibrium flux surface geometry.

B. Momentum balance equations

The momentum balance equation can be written, after subtraction of $m\mathbf{V}$ times the continuity equation, as

$$nm(\mathbf{V} \cdot \nabla)\mathbf{V} + \nabla p + \nabla \cdot \mathbf{\Pi} = ne(\mathbf{E} + \mathbf{V} \times \mathbf{B}) + \mathbf{F} + (\mathbf{S}^1 - m\mathbf{V}S^0), \quad (17)$$

where \mathbf{F} and \mathbf{S}^1 represent interspecies collisional friction and external momentum sources (e.g., neutral beams) or sinks (e.g., charge exchange), respectively, S^0 represents particle sources (e.g., neutral beam and ionization) or sinks (e.g., recombination and ionization to a higher charge state) and the other terms are standard.

In axisymmetric geometry ($\partial/\partial\phi=0$), the toroidal component of Eq. (17) is

$$nm[(\mathbf{V} \cdot \nabla)\mathbf{V}]_\phi + [\nabla \cdot \mathbf{\Pi}]_\phi = ne(E_\phi^A + V_r B_\theta) + F_\phi + (S_\phi^1 - mV_\phi S^0), \quad (18)$$

the poloidal component is

$$nm[(\mathbf{V} \cdot \nabla)\mathbf{V}]_\theta + \frac{1}{h_\theta} \frac{\partial p}{\partial \theta} + [\nabla \cdot \mathbf{\Pi}]_\theta = ne(E_\theta - V_r B_\phi) + F_\theta + (S_\theta^1 - mV_\theta S^0), \quad (19)$$

and the radial component is

$$nm[(\mathbf{V} \cdot \nabla)\mathbf{V}]_r + \frac{1}{h_r} \frac{\partial p}{\partial r} + [\nabla \cdot \mathbf{\Pi}]_r = ne(E_r + V_\theta B_\phi - V_\phi B_\theta) + F_r + (S_r^1 - mV_r S^0). \quad (20)$$

The representation of the differential operators on the left in the Miller flux surface geometry is given in Secs. IV C and IV D.

C. Inertial force

Using Eq. (12) the directional derivative components of the inertial force term can be written as

$$[(\mathbf{V} \cdot \nabla)\mathbf{V}]_\phi = \left(\frac{V_r}{h_r} \frac{\partial V_\phi}{\partial r} + \frac{V_\phi V_r}{h_\phi h_r} \frac{\partial h_\phi}{\partial r} \right) + \left(\frac{V_\theta}{h_\theta} \frac{\partial V_\phi}{\partial \theta} + \frac{V_\phi V_\theta}{h_\phi h_\theta} \frac{\partial h_\phi}{\partial \theta} \right), \quad (21a)$$

$$[(\mathbf{V} \cdot \nabla)\mathbf{V}]_\theta = \left[\frac{V_r}{h_r} \frac{\partial V_\theta}{\partial r} + \frac{V_\theta V_r}{h_\theta h_r} \left(\frac{\partial h_\theta}{\partial r} - \frac{\partial h_r}{\partial \theta} \right) \right] + \frac{V_\theta}{h_\theta} \frac{\partial V_\theta}{\partial \theta} - \frac{V_\theta V_\phi}{h_\theta h_\phi} \frac{\partial h_\phi}{\partial \theta}, \quad (21b)$$

$$[(\mathbf{V} \cdot \nabla)\mathbf{V}]_r = \frac{V_r}{h_r} \frac{\partial V_r}{\partial r} + \left[\frac{V_\theta}{h_\theta} \frac{\partial V_r}{\partial \theta} + \frac{V_r V_\theta}{h_r h_\theta} \left(\frac{\partial h_r}{\partial \theta} - \frac{\partial h_\theta}{\partial r} \right) \right] - \frac{V_r V_\phi}{h_r h_\phi} \frac{\partial h_\phi}{\partial r}. \quad (21c)$$

The metric derivatives of the Miller equilibrium metric elements needed to evaluate Eqs. (21) are

$$\frac{\partial h_\theta}{\partial r} = \sqrt{\cos^2(\theta+x \sin \theta)+\kappa^2 \sin^2 \theta},$$

$$\frac{\partial h_\phi}{\partial r} = \frac{\partial R_0(r)}{\partial r} + \cos(\theta+x \sin \theta),$$

$$\frac{\partial h_r}{\partial \theta} = \frac{\partial(|\nabla r(r, \theta)|^{-1})}{\partial \theta},$$

$$\frac{\partial h_\phi}{\partial \theta} = -r \sin(\theta+x \sin \theta)(1+x \cos \theta).$$

D. Viscous force

1. Toroidal

Using Eqs. (13) and (14) the components of the toroidal viscous force in the Miller flux surface geometry are

$$(\nabla \cdot \mathbf{\Pi})_\phi = \left[\frac{1}{Rh_\phi h_r} \frac{\partial}{\partial r} (Rh_\theta \pi_{r\phi}) + \frac{1}{Rh_r} \frac{\partial R}{\partial r} \pi_{r\phi} \right] + \left[\frac{B_\theta}{h_\theta} \frac{\partial}{\partial \theta} \left(\frac{\pi_{\theta\phi}}{B_\theta} \right) + \frac{1}{Rh_\theta} \frac{\partial R}{\partial \theta} \pi_{\theta\phi} \right]. \quad (23)$$

Specializing the general form of the viscous fluxes derived from Braginskii's⁴ decomposition of the rate-of-strain tensor, generalized to arbitrary curvilinear geometry,⁶ to the Miller equilibrium flux surface geometry yields

$$\pi_{r\phi} = \pi_{\phi r} = -\eta_4 R \frac{1}{h_\theta} \frac{\partial(V_\phi R^{-1})}{\partial \theta} - \eta_2 R \frac{1}{h_r} \frac{\partial(V_\phi R^{-1})}{\partial r}, \quad (24)$$

$$\pi_{\theta\phi} = \pi_{\phi\theta} = -\frac{3}{2} \eta_0 f_p A_0 + \eta_4 R \frac{1}{h_r} \frac{\partial(V_\phi R^{-1})}{\partial r} - \eta_2 R \frac{1}{h_\theta} \frac{\partial(V_\phi R^{-1})}{\partial \theta},$$

with η_n being viscosity coefficients discussed below, $f_p \equiv B_\theta/B_\phi$ and where

$$A_0 = 2 \left\{ -\frac{1}{3h_\theta} \frac{\partial V_\theta}{\partial \theta} + \left[\frac{1}{Rh_\theta} \frac{\partial R}{\partial \theta} + \frac{1}{3B_\theta h_\theta} \frac{\partial B_\theta}{\partial \theta} \right] V_\theta + f_p R \frac{1}{h_\theta} \frac{\partial(V_\phi R^{-1})}{\partial \theta} \right\}. \quad (25)$$

2. Poloidal

Repeating the same procedure for the poloidal components of the viscous force and the viscous fluxes leads to

$$(\nabla \cdot \Pi)_\theta = \frac{1}{H} \frac{\partial}{\partial r} (Rh_\theta \pi_{r\theta}) + \frac{1}{H} \frac{\partial}{\partial \theta} (h_r h_\phi \pi_{\theta\theta}) - \frac{1}{h_\theta h_r} \frac{\partial h_r}{\partial \theta} \pi_{rr} + \frac{1}{h_\theta h_r} \frac{\partial h_\theta}{\partial r} \pi_{\theta r} - \frac{1}{Rh_r} \frac{\partial R}{\partial \theta} \pi_{\phi\phi}, \quad (26)$$

where

$$\begin{aligned} \pi_{r\theta} = \pi_{\theta r} = & -\eta_3 (RB_\theta)^{-1} \frac{1}{h_\theta} \frac{\partial (RB_\theta V_\theta)}{\partial \theta} \\ & - (\eta_4 - \eta_3) f_p \frac{R}{h_\theta} \frac{\partial (V_\phi R^{-1})}{\partial \theta} - \eta_1 \frac{h_\theta}{h_r} \frac{\partial (V_\theta h_\theta^{-1})}{\partial r} \\ & - (\eta_2 - \eta_1) f_p \frac{R}{h_r} \frac{\partial (V_\phi R^{-1})}{\partial r}, \\ \pi_{\theta\theta} = & \frac{1}{2} \eta_0 A_0 + \eta_3 \frac{h_\theta}{h_r} \frac{\partial (V_\phi R^{-1})}{\partial r} + (2\eta_4 - \eta_3) f_p \frac{1}{h_\theta} \frac{\partial (V_\phi R^{-1})}{\partial \theta} \\ & - \eta_1 (RB_\theta)^{-1} \frac{1}{h_\theta} \frac{\partial (RB_\theta V_\theta)}{\partial \theta} + (\eta_1 - 2\eta_2) f_p \frac{R}{h_\theta} \frac{\partial (V_\phi R^{-1})}{\partial \theta}, \\ \pi_{rr} = & \frac{1}{2} \eta_0 A_0 + \eta_1 \left[(RB_\theta)^{-1} \frac{1}{h_\theta} \frac{\partial (RB_\theta V_\theta)}{\partial \theta} - f_p \frac{R}{h_\theta} \frac{\partial (V_\phi R^{-1})}{\partial \theta} \right] \\ & - \eta_3 \left[\frac{h_\theta}{h_r} \frac{\partial (V_\theta h_\theta^{-1})}{\partial r} - f_p \frac{R}{h_r} \frac{\partial (V_\phi R^{-1})}{\partial r} \right], \\ \pi_{\phi\phi} = & -\eta_0 A_0 - 2\eta_4 f_p \frac{R}{h_r} \frac{\partial (V_\phi R^{-1})}{\partial r} + 2\eta_2 f_p \frac{R}{h_\theta} \frac{\partial (V_\phi R^{-1})}{\partial \theta}. \end{aligned} \quad (27)$$

3. Radial

The radial component of the viscous force is derived in the same way, resulting in

$$(\nabla \cdot \Pi)_r = \frac{1}{H} \frac{\partial}{\partial r} (Rh_\theta \pi_{rr}) + \frac{1}{H} \frac{\partial}{\partial \theta} (h_r h_\phi \pi_{\theta r}) + \frac{1}{h_\theta h_r} \frac{\partial h_r}{\partial \theta} \pi_{r\theta} - \frac{1}{h_\theta h_r} \frac{\partial h_\theta}{\partial r} \pi_{\theta\theta} - \frac{1}{Rh_r} \frac{\partial R}{\partial r} \pi_{\phi\phi}. \quad (28)$$

4. Ordering

We note that the Braginskii expressions for the viscous fluxes were developed for a collisional large rotation ($V_\phi \sim V_{th}$) ordering. The extension of the viscosity coefficients to account for lower collisionality (neoclassical) effects is discussed in Sec. IV E. There are also viscous fluxes driven by ion thermal fluxes that become important in the small rotation ($V_\phi \ll V_{th}$) ordering.⁷⁻⁹ This ‘‘thermal’’ viscous flux formalism is presently being worked out in the notation of this paper for comparison with experiment and will be published in a subsequent paper.

E. Viscosity coefficients

The Braginskii expressions⁴ for the ion viscosity coefficients in a collisional plasma are

$$\begin{aligned} \eta_0 = 0.96nT\tau, \quad \eta_1 = \frac{3}{10} \frac{nT}{\Omega^2 \tau}, \quad \eta_2 = 4\eta_1, \\ \eta_3 = \frac{1}{2} \frac{nT}{\Omega}, \quad \eta_4 = 2\eta_3, \end{aligned} \quad (29)$$

where $\tau \sim 10^{-5}$ s is the ion-ion collision time and $\Omega \sim 10^8$ s⁻¹ is the ion gyrofrequency. The classical Braginskii ‘‘parallel’’ viscosity (η_0), ‘‘gyroviscosity’’ ($\eta_{3,4}$), and ‘‘perpendicular’’ viscosity ($\eta_{1,2}$) coefficients are in the ratio $1/(\Omega\tau)^{-1}/(\Omega\tau)^{-2} \approx 1/10^{-3}/10^{-6}$ for a collisional plasma. The form of the gyroviscosity does not depend on collisionality, and the neoclassical effect of lower collisionality on the perpendicular viscosity has been found^{10,11} to be small. On the other hand, the neoclassical effect of lower collisionality on the parallel viscosity coefficient is significant; a representative neoclassical expression is given by¹²

$$\eta_0 = \frac{nmv_{th}qR_0\varepsilon^{-3/2}\nu^*}{(1+\varepsilon^{-3/2}\nu^*)(1+\nu^*)}, \quad (30)$$

where $\nu^* \equiv qR_0/v_{th}\tau$ and $\varepsilon \equiv r/R_0$.

F. Energy balance equation

The fluid energy balance equation is

$$\nabla \cdot \mathbf{Q} = ne\mathbf{V} \cdot \mathbf{E} + R^2 + S^2, \quad (31)$$

where the first term on the right represents Ohmic heating, the second term represents interspecies collisional heating or cooling, the last term represents external heating (e.g., neutral beam or rf), and the total heat flux

$$\mathbf{Q} = \frac{1}{2} nmV^2 \mathbf{V} + \frac{5}{2} nT \mathbf{V} + \mathbf{V} \cdot \Pi + \mathbf{q} \quad (32)$$

consists of a first term representing the convection of kinetic energy, a second term representing the convection of internal energy plus the work done by the flowing plasma against the pressure, a third term representing viscous heating of the plasma by the flows, and a fourth term representing the conduction of internal energy.

Using the previous results, the divergence of the heat flux can be represented in the Miller equilibrium flux surface geometry as

$$\begin{aligned} \nabla \cdot \mathbf{Q} = & \frac{1}{h_r} \frac{\partial}{\partial r} (Q_r) + \frac{Q_r}{h_r} \left(\frac{1}{h_\phi} \frac{\partial h_\phi}{\partial r} + \frac{1}{h_\theta} \frac{\partial h_\theta}{\partial r} \right) + \frac{1}{h_\theta} \frac{\partial}{\partial \theta} (Q_\theta) \\ & + \frac{Q_\theta}{h_\theta} \left(\frac{1}{h_\phi} \frac{\partial h_\phi}{\partial \theta} + \frac{1}{h_r} \frac{\partial h_r}{\partial \theta} \right), \end{aligned} \quad (33)$$

where

$$\begin{aligned} Q_x = & \frac{1}{2} nmV^2 V_x + \frac{5}{2} nTV_x + (V_r \Pi_{rx} + V_\theta \Pi_{\theta x} + V_\phi \Pi_{\phi x}) \\ & + q_x, \quad x = r, \theta. \end{aligned} \quad (34)$$

V. COMPARISON OF CONDUCTIVE HEAT FLUX CALCULATED ON MILLER EQUILIBRIUM FLUX SURFACES AND ON FLUX SURFACES CALCULATED FROM NUMERICAL SOLUTION OF THE GRAD-SHAFRANOV EQUATION

Assuming that the density, temperature, and thermal diffusivity are uniform over the flux surface, the poloidal dependence of the conductive heat flux must arise through the poloidal dependence of the radial temperature gradient

$$\begin{aligned} q_r(r, \theta) &= n(r)T(r)\chi(r)L_T^{-1}(r, \theta) \\ &= n(r)T(r)\chi(r)\langle L_T^{-1}(r) \rangle \left[\frac{|\nabla r(r, \theta)|}{\langle |\nabla r(r)| \rangle} \right] \\ &\equiv \langle q_r(r) \rangle \left[\frac{|\nabla r(r, \theta)|}{\langle |\nabla r(r)| \rangle} \right], \end{aligned} \quad (35)$$

where $|\nabla r|$ is given by Eq. (2), the symbol $\langle A \rangle$ denotes the FSA of the quantity A defined by Eq. (7), and $L_T^{-1} \equiv -(\mathbf{n}_r \cdot \nabla T)/T$ is the temperature radial gradient scale length. For the sake of comparison, the poloidal distribution of the conductive radial heat flux about 6 cm (at the outboard midplane) inside the separatrix in a DIII-D discharge has been calculated in two ways: (1) the energy balance equation (31) was solved numerically for $q_r(r, \theta)$ in two-dimensional (2D) flux surface geometry determined from the numerical solution of the Grad-Shafranov equation, and (2) the flux surface averaged $\langle q_r(r) \rangle$ was calculated from a one-dimensional flux surface averaged energy balance equation and then Eqs. (2) and (7) were used to evaluate $q_r(r, \theta)$ using the last form of Eq. (35). The calculations used experimental densities and temperatures, and were intercalibrated so that the flux surface averaged $\langle q_r(r) \rangle$ were very similar for all calculations so that the comparison actually compares how well the Miller equilibrium calculation of $|\nabla r(r, \theta)|/\langle |\nabla r(r)| \rangle$ from Eqs. (2) and (7) compares with direct numerical solution for the poloidal distribution of the radial conductive heat flux.

The comparison of $q_r(r, \theta)/\langle q_r(r) \rangle$ is shown in Fig. 4. Two 2D numerical flux surface calculations are shown, one with the SOLPS code¹³ and one with the UEDGE code¹⁴ (which calculated the ratio of local to flux surfaced average total heat flux). Two versions of the Miller equilibrium calculation are also shown, one in which the average experimental triangularity and elongation were used at all poloidal locations (labeled “sym”) and the other in which separate experimental triangularities and elongations were used in the upper and lower regions to take into account the effect of the lower divertor (labeled “asym”).

VI. SUMMARY AND CONCLUSION

The “Miller equilibrium” is an analytical solution to the Grad-Shafranov equation, which represents the magnetic flux surfaces in terms of the elongation κ , the triangularity δ , and the location of displaced centers $R_0(r)$. The metrics for a flux surface coordinate system using this analytical solution are presented, and the plasma fluid equations are explicitly represented in this flux surface coordinate system. Solving

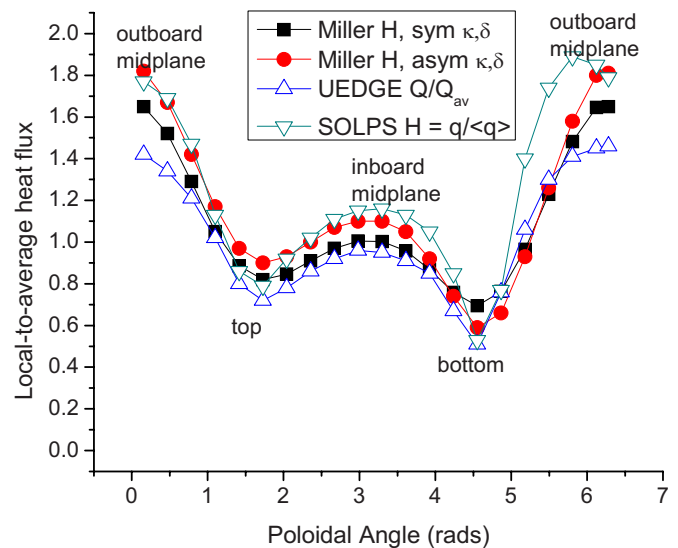


FIG. 4. (Color online) Predicted poloidal distribution of the conductive energy flux just inside the separatrix for a DIII-D shot. [Reprinted from Ref. 15, W. M. Stacey, *Phys. Plasmas* **15**, 122505 (2008). Copyright © 2008 American Institute of Physics.]

this set of fluid equations is equivalent to, but should be more efficient computationally than, the usual “1.5D transport” solution procedure in which the Grad-Shafranov equation is first solved numerically to establish the flux surface coordinate system that is then used for the solution of the fluid equations.

ACKNOWLEDGMENTS

This work was supported by the U.S. Department of Energy Grant No. DE-FG02-00-ER54538 with the Georgia Tech Research Corporation.

- ¹R. L. Miller, M. S. Chu, J. M. Greene, Y. R. Lin-Liu, and R. E. Waltz, *Phys. Plasmas* **5**, 973 (1998).
- ²L. L. Lao, S. P. Hirshman, and J. Wieland, *Phys. Fluids* **24**, 1431 (1981).
- ³P. M. Morse and H. Feshbach, *Methods of Theoretical Physics* (McGraw-Hill, New York, 1953), pp. 21–30.
- ⁴S. I. Braginskii, *Rev. Plasma Phys.* **1**, 205 (1965).
- ⁵W. M. Stacey, *Fusion Plasma Physics* (Wiley-VCH, Weinheim, 2005), pp. 85–100.
- ⁶W. M. Stacey and D. J. Sigmar, *Phys. Fluids* **28**, 2800 (1985).
- ⁷A. B. Mikhailovskii and V. S. Tsypin, *Sov. J. Plasma Phys.* **10**, 51 (1984).
- ⁸H. A. Claassen, H. Gerhauser, and A. Rogister, *Phys. Plasmas* **7**, 3699 (2000).
- ⁹P. J. Catto and A. Simakov, *Phys. Plasmas* **11**, 90 (2004); **12**, 012501 (2005).
- ¹⁰F. L. Hinton and S. K. Wong, *Phys. Fluids* **28**, 3082 (1985).
- ¹¹J. W. Connor, S. C. Cowley, R. J. Hastie, and L. R. Pan, *Plasma Phys. Controlled Fusion* **29**, 919 (1987).
- ¹²W. M. Stacey, A. W. Bailey, D. J. Sigmar, and K. C. Shaing, *Nucl. Fusion* **25**, 463 (1985).
- ¹³V. A. Rozhansky, S. P. Voskoboinikov, E. G. Kaveeva, D. P. Coster, and R. Schneider, *Nucl. Fusion* **41**, 387 (2001); **42**, 1110 (2002); **43**, 614 (2003); *Contrib. Plasma Phys.* **46**, 575 (2006).
- ¹⁴T. D. Rognlien, D. D. Ryutov, N. Mattor, and G. D. Porter, *Phys. Plasmas* **6**, 1851 (1999); T. D. Rognlien and D. D. Ryutov, *Contrib. Plasma Phys.* **38**, 152 (1998); T. D. Rognlien, *Plasma Phys. Controlled Fusion* **47**, A283 (2005).
- ¹⁵W. M. Stacey, *Phys. Plasmas* **15**, 122505 (2008).